Physica Scripta

Laser cooling of relativistic heavy-ion beams for FAIR

IOP Publishing | Royal Swedish Academy of Sciences Physica Scripta

Phys. Scr. T166 (2015) 014048 (6pp) doi:10.1088/0031-8949/2015/T166/014048

Laser cooling of relativistic heavy-ion beams for FAIR

D Winters[1], T Beck[2], G Birkl[2,10], C Dimopoulou[1], V Hannen[3], Th Kühl[1,4,5], M Lochmann[1,4], M Loeser[6,7,10], X Ma[8,11], F Nolden[1], W Nörtershäuser[1,2,4,10], B Rein[2], R Sánchez[1], U Schramm[6,7,10], M Siebold[6], P Spiller[1], M Steck[1], Th Stöhlker[1,5,9], J Ullmann[2,5], Th Walther[2,10], W Wen[6,8,10,11,12], J Yang[8,11], D Zhang[8,11] and M Bussmann[6]

[1] GSI Darmstadt, Germany
[2] TU Darmstadt, Germany
[3] Münster University, Germany
[4] Mainz University, Germany
[5] Helmholtz Institute Jena, Germany
[6] Helmholtz-Zentrum Dresden—Rossendorf, Germany
[7] Technische Universität Dresden, Germany
[8] IMP-CAS Lanzhou, People's Republic of China
[9] Jena University, Germany

E-mail: d.winters@gsi.de

Received 16 February 2015, revised 27 July 2015
Accepted for publication 14 August 2015
Published 26 November 2015

Abstract

Laser cooling is a powerful technique to reduce the longitudinal momentum spread of stored relativistic ion beams. Based on successful experiments at the experimental storage ring at GSI in Darmstadt, of which we show some important results in this paper, we present our plans for laser cooling of relativistic ion beams in the future heavy-ion synchrotron SIS100 at the Facility for Antiproton and Ion Research in Darmstadt.

Keywords: laser cooling, heavy ions, relativistic beams, highly charged ions, FAIR

(Some figures may appear in colour only in the online journal)

1. Introduction

Stored ion beams with a very small longitudinal momentum spread $\Delta p/p$ and small emittance ϵ are of great interest for many atomic and nuclear physics experiments. Usually, such high-quality beams are obtained by means of electron cooling [1] and/or stochastic cooling [2]. These are very powerful and reliable methods, as has been demonstrated during numerous experiments in recent decades. For low-energy ($\gamma \sim 1$) storage rings, which are typically small in size (circumference $\sim$50 m), often electron cooling is available. At much higher energies ($\gamma > 5$, circumference $>$500 m), electron cooling becomes less effective, which results in longer cooling times (see e.g. [3]). Also, in order to reach such highly relativistic velocities, a very sophisticated electron cooler would have to be built, implying high costs and great technological challenges. This would, for instance, also be the case for the heavy-ion synchrotron SIS100 at the future Facility for Antiproton and Ion Research (FAIR) in Darmstadt [4].

Therefore, another technique was considered: laser cooling of stored ion beams. Laser cooling of stored *coasting* ion beams was first demonstrated at the TSR in Heidelberg (Germany) [5], and at ASTRID in Aarhus (Denmark) [6]. Laser cooling of stored *bunched* ion beams was demonstrated a few years later at ASTRID [7], followed by studies at the TSR [8, 9]. Experiments on laser-cooled ion crystal structures were performed in circular Paul traps [10] while ion beam crystallization was studied at the table top storage ring PALLAS [11, 12] in Munich (Germany). At the experimental

[10] Work supported by BMBF.
[11] Work supported by BMBF-WTZ.
[12] Work supported by DAAD.

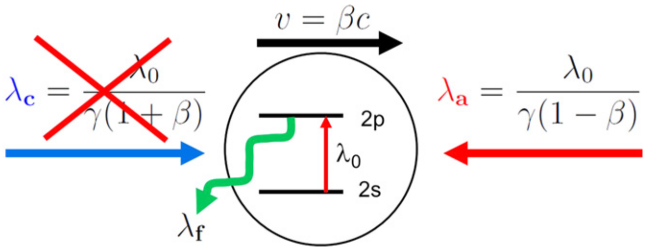

Figure 1. The principle of laser cooling: the ion absorbs a photon—thus momentum—from a counter-propagating laser beam, and deexcites by fluorescence. The counteracting force, required for laser cooling, is provided by the 'rf-bucket', which comes from *bunching* the ion beam.

storage ring (ESR) in Darmstadt (Germany), first laser cooling experiments with relativistic ion beams [13] were conducted. Transverse laser cooling has been studied in detail at the S-LSR [14] in Kyoto (Japan). At the CSRe [15] in Lanzhou (China) experiments with relativistic ion beams have been started. For a good review of the topic, see [16].

In this paper we will try to make the transition from laser cooling at the heavy-ion storage ring ESR to laser cooling at the heavy-ion synchrotron (SIS100). Firstly, the principle of laser cooling of stored, bunched, relativistic ion beams will be briefly discussed. Then, a short overview of the important experimental work (setup, results) at the ESR—relevant for future laser cooling at the SIS100—will be given. Finally, our plans for the SIS100 will be presented, starting with a description of the machine, followed by the experimental setup, and ending with possible first experiments.

2. Laser cooling of stored, bunched, relativistic ion beams

The 'classical' laser force results from the scattering (i.e. absorption and subsequent emission) of laser photons from an ion via a fast atomic transition. The absorbed laser photons, and thus their momentum, come from a single direction and their wavelength must match the Doppler-shifted *cooling transition* in the ion. Fluorescence emission, and thus recoil, occurs in all directions and averages out to zero, leaving a net cooling force in the direction of the laser light. Figure 1 schematically shows the method for a 2s → 2p ($E1$) transition. In this anti-collinear geometry, the required laser wavelength scales extremely favourably with γ. For this geometry, the equation describing the 'Doppler relationship' between the wavelength (λ_0) in the rest frame of the moving ion, and that of the anti-collinear laser (λ_a) in the lab frame is given by

$$\lambda_a = \frac{\lambda_0}{\gamma(1-\beta)}, \text{ where } \gamma = \frac{1}{\sqrt{1-\beta^2}} \text{ and } \beta = \frac{v}{c}. \quad (1)$$

Here, v is the velocity of the ion, and c the speed of light in vacuum. For example, to reach the 2s → 2p transition in C^{3+} (155 nm) at 47% of c in an anti-collinear geometry, a laser system with $\lambda_a = 257$ nm is required. A collinear geometry would require a laser wavelength of $\lambda_c = 93$ nm, which already demonstrates that such an approach to counterbalance the cooling laser does not favourably scale with γ. Therefore, the *rf-bucket* force, which comes from bunching the ion beam, is the better and certainly more general counterpart to the laser force [16]. The fluorescence wavelength (λ_f), measured in the lab frame, is also modified by the Doppler effect. For highly charged ions at velocities close to c, the relativistic effects of both the motion (i.e. the Doppler effect) and the properties of the ion (i.e its electronic structure) need to be considered. These effects complicate the description of the laser cooling force, and strongly affect the fluorescence emission and the required laser intensity [17]. It is also important to choose a transition with a lifetime much shorter than the revolution time of the ions in the ring, as the total cooling force is given by the momentum transfer of the photon to the ion multiplied by the scattering rate, which is fundamentally limited by the lifetime of the transition. In turn, this means that in a standard accelerator the photon scattering rate can easily be several hundreds of kHz per ion.

The Lorentz factor γ can conveniently be expressed in terms of a particular circular accelerator, specified by its magnetic rigidity ($B\rho$), and the properties of the ion, specified by its charge Q and mass M, i.e. $\gamma = f(B\rho, Q, M)$. This equation is extremely practical and reads in full:

$$\gamma = \sqrt{\left(\frac{B\rho Q}{Mc}\right)^2 + 1}\,, \text{ where } Q = q \cdot e \text{ and } M = m \cdot u. \quad (2)$$

Here, q is the charge state of the ion, e the elementary charge, m the atomic weight, and u the unified atomic mass unit. The magnetic rigidity of a storage ring determines the maximum energy at which a beam of ions of a given mass-to-charge ratio can be stored.

3. Laser cooling at the ESR

There have been three beamtimes for laser cooling of $^{12}C^{3+}$ ions at the ESR: in 2004, in 2006, and in 2012. These beamtimes focussed on determining, understanding and controlling the parameters for effective laser cooling. The γ-value for these experiments is obtained by inserting $B\rho = 6.6$ Tm, $q = 3$, and $m = 12$ in equation (2), yielding $\gamma \approx 1.13$ (and $\beta \approx 0.47$). The kinetic energy of the ion is given by $E_{kin} = (\gamma - 1)Mc^2 = 122$ MeV u^{-1}. These experiments were performed using laser systems with a wavelength of 257 nm, a moderately bunched ion beam, and standard ion beam diagnostics. The ion beam was bunched by applying a low rf-voltage ($\sim V$) to the exciter at a frequency ($f_b = h \cdot f$) given by the product of the harmonic number $h = 5$–20 and the ion revolution frequency ($f \sim 1$ MHz). We note that bunching using a resonant rf-cavity was disfavored in all experiments, because the applied voltages were too low and the rf-frequencies too high for resonant cavities. Instead, exciter electrodes, which are simple parallel plates carrying an rf-current, were used to create an rf-bucket force comparable to the laser cooling force of a few eV mm^{-1}.

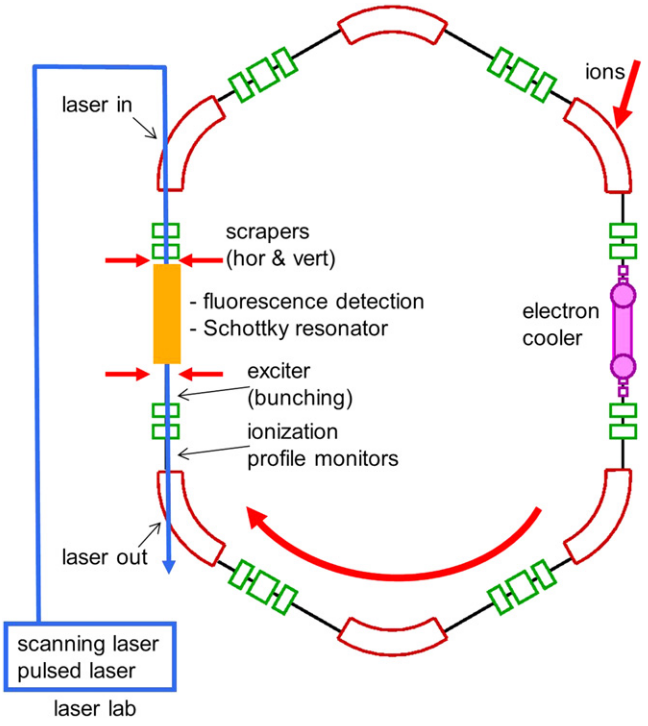

Figure 2. The experimental storage ring (ESR) at GSI. The ions enter from the top right, orbit in a clockwise direction, and face the laser photons in the straight section on the left. Here, also the laser light is coupled in and out of the vacuum, and revolution frequency, position, and fluorescence of the ions are measured.

The experimental setup from the 2012 beamtime is schematically shown in figure 2. The laser lab is separated from the storage ring facility, because permanent access and appropriate air conditioning (dust, temperature) is required. The laser light had to be transported over long distances, i.e. of the order of 60 m, which meant that laser beam pointing and stabilization were important issues. It was not possible to transport the laser light through an evacuated beamline, which limited and reduced (due to losses in air and dust on mirrors) the maximum laser power and minimum wavelength of the UV-laser and especially led to strong distortions in the beam profile due to air convection. The laser light then entered the ESR-vacuum through a UV-grade quartz window, after which the spatial overlap between ion and laser beams was adjusted using horizontal and vertical 'scrapers'. These are metal plates that can be precisely (0.1 mm resolution) moved inside the vacuum to determine the position of ion and laser beam. At the zero-position, the edge of the scrapers coincides with the center of the ion beam, which allows to adjust the laser beam without the ion beam. When pulsed laser systems are used, also overlap in time is required, synchronizing the laser pulses to the bunching frequency and thus the arrival of the ion bunches. The set of diagnostics used was rather large, enabling us to measure the revolution frequency of the stored ions (Schottky resonator [18]), the position and width of the ion beam (ionization profile monitors), and the fluorescence from the ions (*ex-vacuo* UV-sensitive photomultiplier tubes and *in-vacuo* UV-photochanneltron detectors). Unfortunately, only little fluorescence was detected, even by the *in-vacuo*

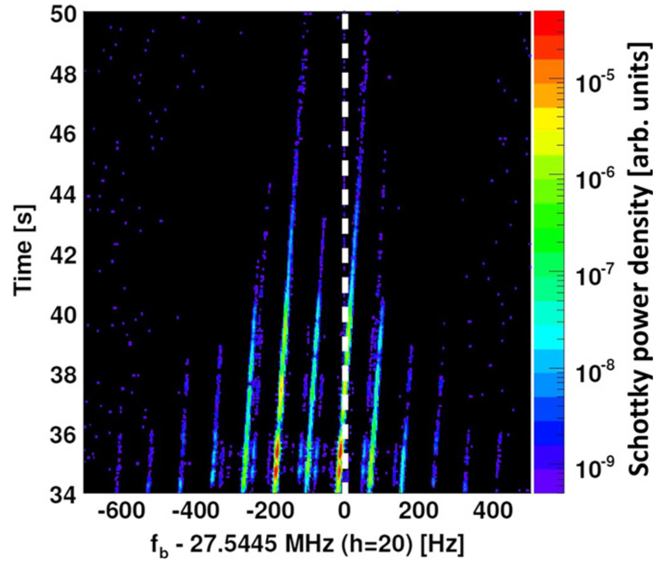

Figure 3. Result from the ESR beamtime in 2006: the cw laser is at a fixed wavelength and the bunching frequency is changed. The slanted equidistant straight lines are due to synchrotron oscillations of the ions of varying amplitude inside the bucket [19]. The width of this distribution of sidebands determines the relative momentum spread.

detectors, so that more development is required for future experiments.

During these ESR beamtimes, two schemes for laser cooling were studied. The beamtimes in 2004 and 2006 used a fixed cw-laser system and the bunching frequency was scanned continuously [19]. The result of this scheme is shown in figure 3, where time is plotted along the vertical axis, increasing from bottom to top, and a high-order harmonic of the ion's revolution frequency (1.3 MHz) on the horizontal axis, increasing from left to right. The logarithmic color scale represents the Schottky power density (red = high, blue = low). The slanted lines correspond to the different synchrotron sidebands of the ion motion inside the rf-bucket. As time progresses, the bunching frequency is scanned (indicated by the slanted lines). During this scan, the laser is *red detuned* and only interacts with ions of a particular velocity class, which are in resonance with the laser. Thereby, the momentum spread of the beam is steadily decreasing, as indicated by the disappearance of the outer synchrotron sidebands during the scan. When only the central lines are seen, the ion beam is the coldest and the $\Delta p/p$ value, determined by a Gaussian fit to the envelope of the synchrotron sidebands, reaches a minimum ($<10^{-6}$) set by the measurement method itself. At this particular harmonic, the Schottky power density vanishes for bunched ion beams [19]. When the bunching frequency is detuned further, the laser light crosses the transition frequency of the ion. After this point (not shown), the laser becomes *blue detuned* implying that the force has changed its sign. The laser force then points in the same direction as the bucket force and resonantly drives the ion motion inside the rf-bucket causing a strong heating of the ion bunch. At the end of each scan, the bunching frequency is reset and a new cooling phase begins.

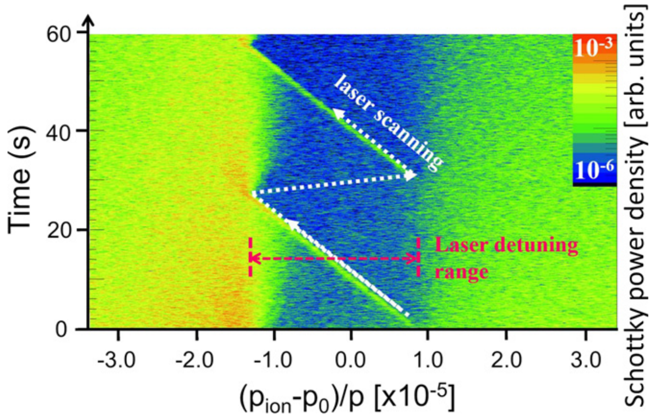

Figure 4. Result from the ESR beamtime in 2012: a cw laser is scanned over a broad frequency range, consecutively interacting with the ions inside a coasting beam. The logarithmically colour-coded Schottky power density shows that ions within the scanning range are decelerated to lower momenta by the laser force, leaving the revolution frequency range covered by the laser scan depopulated of ions [20].

During the 2012 beamtime [20, 21], a tuneable cw-laser system was used, which could quickly ($\ll$1 s) scan over a very broad range (several tens of GHz) [22]. This had the great advantage that the bunching frequency could be fixed. Although this technique has been used before at lower energies, here it was first applied to relativistic energies [23]. When the ions move at velocities close to *c*, their absolute velocity spread is usually much larger than at lower velocities. This, in principle, increases the probability for the ions to overcome the laser force, as a few scattering events only might not be sufficient to slow down the ions such that they can interact more than once with the laser while scanning. Such ions would then move out of resonance and would no longer be cooled. Fortunately, first results depicted in figure 4, using a scanning laser and a coasting ion beam (no bunching, no electron cooling), indicated that this is seldomly the case and, indeed, the laser can effectively decelerate the ions. From figure 4 it can be seen that consecutive scanning of the laser reduces the amount of ions at higher revolution frequencies, decelerating them to lower ones. This leaves the scanning region void of ions, indicating that only a small number of ions can overcome the laser cooling force and is not decelerated. It should be noted that, different to a coasting beam, ions in a bunched beam oscillating in the bucket can interact with the laser more than once. The results for bunched ion beams are under analysis and will be presented elsewhere.

The 2012 cooling scheme compares favourably to the 2006 scheme, also because previous results indicated that a stepwise scanning of the bunching frequency might excite synchrotron oscillations in the bucket [19]. These are expected to become more severe for the higher bunching voltages required at higher ion beam energies. Moreover, scanning the bunching voltage locally changes the ion beam energy, which is not desirable for high-precision experiments. Ergo, for laser cooling at high energies, it is best to scan the laser frequency and fix the bunching frequency. Novel pulsed laser systems would be even better, enabling simultaneous cooling of many velocity classes due to the huge laser bandwidth. In order to maximize the laser cooling force, the repetition rate of the pulsed laser must be of the order of the ion revolution frequency, and there must be enough power in all bands of the spectrum. The bandwidth and shape of the laser spectrum must be optimized to the initial momentum spread of the injected ion beam and will require the use of more than one laser pulse and thus synchronisation.

4. Laser cooling at the SIS100

The success of laser cooling at the ESR encouraged us to consider this method for the SIS100. Due to the very large $B\rho$-range (9–100 Tm), an equally large Doppler-range can be exploited, offering possibilities for laser cooling of many different heavy highly charged ions [24]. This can be understood via equations (1) and (2), which are fully relativistic and therefore hold in general. As an example, we consider a heavy ion such as Sn ($Z = 50$, $m \approx 119$) in a Li-like charge state ($q = 47$). The mass-to-charge ratio is then $m/q \approx 2.5$. According to equation (2), for $B\rho = 100$ Tm, this yields $\gamma \approx 13$. From equation (1) it can then be inferred that a laser with $\lambda_a = 257$ nm reaches a transition wavelength of $\lambda_0 \approx 10$ nm, which corresponds to a $2s_{1/2} \rightarrow 2p_{1/2}$ transition in this ion. This example clearly demonstrates the very large range of transition wavelengths accessible using just standard laser systems. At the moment, we are performing a theoretical study [25] covering a very large range of ions in different charge states, in order to see which transitions are possible and which are the most interesting ones for first experiments at the SIS100. These results will be published soon.

For laser cooling at the SIS100, the setup must be similar to that of the ESR, shown in figure 2, and at least contain a laser system, a set of scrapers, a buncher (exciter), and a dedicated fluorescence detection system. A Schottky pick-up or resonator would also be extremely valuable, as can be understood from figures 3 and 4. For spatial overlap, dedicated reference points along the beam tube will allow for reproducible offline positioning of the laser beam relative to the beam tube and thus the ion beam to about 1 mm precision. Figure 5 shows the ring design of the SIS100, the injection of ions, the laser cooling facility (sector 3), the laser lab in the (inner) service tunnel, and the detector lab in the (outer) accelerator tunnel. Details of the FAIR facility can be found in [26]. We like to note that the planned laser cooling facility, as described below, can serve both the SIS100 and the future SIS300, which will be placed directly above the SIS100. All components will therefore be installed at strategic places. The SIS100 will be located underground, about 20 m deep, and will have a circumference of 1084 m, which is ten times that of the ESR. The residual gas pressure inside the SIS100 will be on the 10^{-11} mbar level.

For the laser light to reach the accelerator, it will be transported from the laser lab in the (inner) service tunnel to the (outer) accelerator tunnel, passing through concrete walls

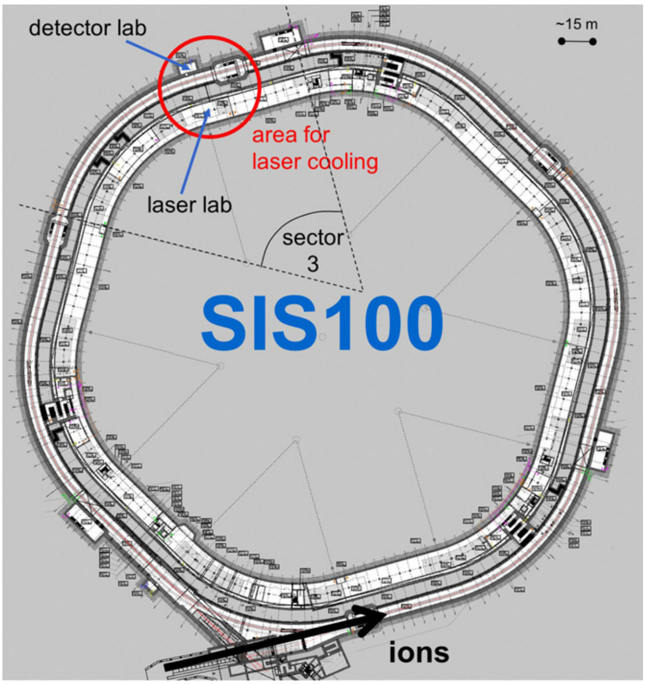

Figure 5. The heavy-ion synchrotron SIS100 at FAIR. The circumference is 1084 m, and the maximum magnetic rigidity is 100 Tm. There will be two tunnels: the inner one is the service tunnel containing the laser lab, and the outer one is the accelerator tunnel. The area for the laser cooling facility is encircled.

and a thick layer of soil between the two tunnels. This laser beamline (length 25 m, diameter 20 cm) should be made out of stainless steel tubes with proper flanges, as these tubes can be evacuated (pressure $\sim 10^{-6}$ mbar). The vacuum has the advantage that laser light covering a very broad spectrum can be transported without considerable loss or distortion, ranging (in wavelength) from the IR ($\lambda \sim \mu$m) down to the XUV range ($\lambda \sim$ nm). The beamline will be equipped with mirror boxes and proper diagnostics at required places. The laser lab (180 m^2) will have (restricted) access at all times, and will contain a special cleanroom (50 m^2) where the laser systems can be operated.

There will also be a detector lab (45 m^2), in which special detector systems for x-ray measurements, such as a crystal spectrometer [27] or a microcalorimeter [28], can be installed. Inevitably, this area is part of the accelerator tunnel and can therefore only be accessed during shutdown periods. Detector systems for the IR- to the XUV-range are, however, still compact and could be installed directly at or close to the SIS100 accelerator. Fluorescence detection at the expected wavelengths is not trivial and requires innovation, simulations, and (depending on the wavelength) different detector systems [29]. Especially at high γ-values, the fluorescence is emitted in a narrow forward cone ('searchlight'), which requires the detection system to be moveable and come very close to the ion beam. Furthermore, when high-intensity ion beams ($\sim 10^{10}$ ions/bunch) are used at extremely high beam energies, estimations of the expected photon flux are required for proper radiation safety measures.

The laser light will be coupled in and out of the accelerator using special vacuum chambers with optics and diagnostics (see figure 2). Then, the spatial overlap between laser and ion beam needs to be adjusted using scrapers and reference points. Because the laser light has to come from the outside, enter the beamline through a special port, and then exit again, the ion beam will have to make a special 'kink' of a few mrad, introducing a dispersion. The length of the spatial overlap will be about 25 m. The overlap in time can be made using the bunch-timing of the accelerator and the timing of the pulsed laser. Finally, the laser focus will be adjusted in order to optimize the fluorescence yield and the cooling time. *Note*: at the SIS100 the overlap region is not field free and close to the beam line, at both ends of the overlap region, magnetic fields could reach up to 1 T. These could potentially have side effects on the atomic levels used for cooling, but are fortunately limited to the small regions close to the ends of the overlap.

The decision for a particular cooling transition (e.g. $2s_{1/2} \rightarrow 2p_{1/2}$) in a particular ion (e.g. Li-like Sn) defines the wavelength (λ_0), the lifetime of the excited state (τ_0), and therefore the saturation intensity (I_{sat}) required for laser cooling. The laser wavelength (λ_a) should then be defined together with the kinetic energy of the ion, hence $B\rho$ and γ. When all these parameters are set, the observed fluorescence wavelength and rate can be determined [24, 25].

First tests with the facility will use available modern laser systems, such as tuneable cw lasers and pulsed lasers, either at 1028, 514, or 257 nm. These laser systems will be provided by the Technical Universities of Darmstadt and Dresden in cooperation with Helmholtz–Zentrum Dresden–Rossendorf, Germany. First ion species will have simple Li-like configurations, where the transitions are either known or can be calculated accurately. Once the facility has passed all the tests, and first laser cooling has been demonstrated, other ion species and/or laser systems will be used. Here we emphasize that, with the same facility, also laser spectroscopy experiments can be performed, because once the cooling transition is found it can also precisely be measured. Ultracold beams are of great interest in itself due to their beam dynamics and possible ordering effects, thus optical diagnostics of the phase space of such beams will be developed to complement standard beam diagnostics. Last, but certainly not least, it will be attempted to extract the laser-cooled ion beams from the SIS100. By pre-bunching and bunch compression, very short ion bunches can be made in the SIS100. When these bunches are laser-cooled and extracted, very cold and very short ultra-relativistic ion bunches can uniquely be delivered to experiments.

References

[1] Budker G I 1967 *Sov. At. Energy* **22** 438
[2] van der Meer S 1972 *CERN/ISR-PO/* 72–31 http://cds.cern.ch/record/312939
[3] Poth H 1990 *Phys. Rep.* **196** 135
[4] Spiller P *et al* 2013 *Proc. IPAC 2013* (*Shanghai, China*) p 3782 THPWO011
[5] Schröder S *et al* 1990 *Phys. Rev. Lett.* **64** 2901

[6] Hangst J S *et al* 1991 *Phys. Rev. Lett.* **67** 1238
[7] Hangst J S *et al* 1995 *Phys. Rev. Lett.* **74** 4432
[8] Lauer I *et al* 1998 *Phys. Rev. Lett.* **81** 2052
[9] Eisenbarth U *et al* 2000 *Nucl. Instrum. Meth. Phys. Res.* A **441** 209
[10] Birkl G *et al* 1992 *Nature* **357** 310
[11] Schätz T *et al* 2001 *Nature* **412** 6848
[12] Schramm U *et al* 2001 *Phys. Rev. Lett.* **87** 184801
[13] Schramm U *et al* 2005 *Proc. PAC 2005* (*Knoxville, USA*) p 401 FOAD004
[14] Noda A *et al* 2005 *Proc. COOL 2007* (*Bad Kreuznach, Germany*) p 221 FRM1I01
[15] Wen W *et al* 2013 *Phys. Scr.* **T156** 014090
[16] Schramm U *et al* 2004 *Prog. Part. Nucl. Phys.* **53** 583
[17] Habs D *et al* 1990 *Proc. ECOOL 1990* (*Legnaro, Italy*) p 122
[18] Nolden F *et al* 2011 *Nucl. Instrum. Methods Phys. Res.* A **659** 69
[19] Bussmann M *et al* 2007 *J. Phys. Conf. Ser.* **88** 012043
[20] Wen W *et al* 2014 *J. Phys. Conf. Ser.* **488** 122005
[21] Bussmann M *et al* 2009 *Proc. COOL 2009* (*Lanzhou, China*) p 22 MOA1MCIO01
[22] Führer T and Walther T 2008 *Opt. Lett.* **33** 372
[23] Winters D *et al* 2013 *Proc. COOL 2013* (*Mürren, Switzerland*) p 166 THAM1HA04
[24] Bussmann M 2014 *ICFA Beam Dynamics Newsletter* vol 65
[25] Shevelko V 2014 private communication
[26] FAIR—Baseline 2006 *Technical Report* GSI
[27] Backe H 2006 *Hyp. Int.* **171** 93
[28] Kraft-Bermuth S *et al* 2015 **T166** 014028
[29] Hannen V *et al* 2013 *JINST* **8** P09018